doi:10.3772/j.issn.1006-6748.2023.01.003

Experimental and numerical investigation of a composite structure with frame and skin①

LI Chuanzheng(李传政)②* **, XU Shuyan*, DONG Jihong*, LIU Bo*, ZHANG Yaoyu*, ZHENG Fusheng***
(* Changchun Institute of Optics, Fine Mechanics and Physics, Chinese Academy of Sciences, Changchun 130033, P. R. China)
(** University of Chinese Academy of Sciences, Beijing 100049, P. R. China)
(*** School of Mechanical and Aerospace Engineering, Jilin University, Changchun 130025, P. R. China)

Abstract

A composite structure with frame and skin based on cabin structure in a large space telescope is studied in this paper. The frame is composed of longitudinal and transverse beams with hybrid bonded/bolted joints, and the skin is connected to the frame by bolts. Tensile tests are conducted on the structure by a set of test stand. It is observed that residual deformation occurs in the first test of the structure, which is attributed to the relative sliding between the skin and frame because of bolt-hole clearances. The high tightening torque and the increased number of the skin-frame bolts contribute to the high stiffness of the structure. A finite element model (FEM) of this composite structure is established, and the simulation model is verified by the experimental results. The FEM is contrastively analyzed with different frame joints, and it is found that adhesive joining in the hybrid bonded/bolted joints enhances the stiffness of the structure significantly. Given that adhesive plays a leading role in the stiffness of the hybrid joints, Tie contact in FEM is proposed to simulate bonded or hybrid joints when studying the stiffness performance of undamaged structure.

Key words: composite, tensile test, hybrid bonded/bolted joint, bolted connection, finite element analysis

0 Introduction

Owing to its advantages of high specific strength, high specific stiffness, and designability of mechanical performance, composite has been applied extensively in the aerospace field from structure with no or minor load to main supporting structure[1-2]. The main supporting structure of large spacecraft usually consists of many separate components connected by joints, which are potential weak points in the structure because of geometry interruptions and discontinuities in materials that tend to produce stress concentration. Thus, joint design is an important aspect of composite structure design[3].

Composite joints can be classified into three types, namely, bonded joint, mechanical joint, and hybrid joint[4]. Mechanical joint usually refers to bolted joint or riveted joint, and hybrid joint usually refers to bonded/bolted joint or bonded/riveted joint. Bonded and mechanical joints are the two most commonly applied types of joints; the former is usually used in parts bearing minor load, and the latter is usually used in parts bearing major load or with high reliability. Hybrid joint is a new connection type that is initially designed to increase the security and redundancy of composite structure. Many investigations have been conducted on composite joints by analytical methods, experimental tests, and numerical simulations[5].

Refs[6-9] used 3D finite element model (FEM) and experimental tests to investigate the effects of bolt-hole clearance on the stiffness and strength of composite bolted joints including single-bolt single-lap joints and multi-bolt double-lap joints; they found that an increased clearance resulted in reduced joint stiffness and increased ultimate strain. Refs[10-11] studied the effects of clamping force, bolt stiffness, and washer size on the response and failure of double-lap bolted composite joints by 3D FEM and experiments. Li et al.[12] made an experimental study on the tensile property of the single-lap composite joints and found that, hybrid joint had the highest tensile strength because the bolts in the hybrid joints could enhance the tensile

① Supported by the National Natural Science Foundation of China (No. 51805510) and Science and Technology Development Plan Project of Jilin Province (No. 20200201294JC).
② To whom correspondence should be addressed. E-mail: nwpulcz@163.com.
Received on Feb. 19, 2022

property after the adhesive failure, while the adhesively bonded joint achieved the lowest strength. Barut and Madenci[13] studied single-lap hybrid (bolted/bonded) joints using a semi-analytical method and observed that the bolt started to take some of the load once the adhesive debond length exceeded a critical length and then took the entire load when full debonding occurred. Lee et al.[14] manufactured and tested 10 hybrid joints and found that the failure loads of hybrid joints were nearly identical to those of adhesive joints and were at least twice as large as those of mechanical joints and the adhesive failure in the hybrid joint occurred before mechanical failure. Kweon et al.[15] tested composite-to-aluminum double lap joints and found that hybrid joining improved joint strength when the mechanical fastening was stronger than the bonding. However, when the bolted joint had lower strength than the bonded joint, bolt joining contributed minimally to the strength of the hybrid joint. Gamdani et al.[16] investigated hybrid bonded/bolted composite joints with up to three bolts and concluded that the adhesive increased the strength of joints, the outer bolts limited the peel stress, and the adhesive reduced the stress concentration around the bolts. Li et al.[17] experimentally and numerically investigated the tensile properties of a composite-metal single lap hybrid bonded/bolted joint and found that the hybrid joint had higher strength and greater initial damage load and tensile stiffness than the pure bolted joint. Zhang[18] used numerical simulation and experiments to study the tensile properties and fatigue life of composite laminates and titanium alloy multi-bolt hybrid joints, and the influence of the number of bolts, bolt arrangement, lap width and other parameters were taken into consideration.

According to the research status on composite joints, most studies selected single lap or double lap joints where shear load is mainly applied as the research objects. Although the strength performance and damage failure of joints have been widely investigated, stiffness performance is not studied synthetically. In engineering practice, the main supporting structure of spacecraft usually contains many complex joints where multiple loads exist. The stiffness performance of spacecraft structure is represented by fundamental frequency which is an important parameter and required to be higher than that of rocket to avoid resonance during launch. In particular, it is highly crucial for large spacecraft with increased mass which tends to reduce the structural stiffness.

In this work, a composite structure with frame and skin based on cabin structure in a large space telescope is studied on stiffness performance. The bolted connections of the skin and frame are studied by comparing with frame only and considering the effects of tightening torques and numbers of skin-frame bolts. The connections of frame are studied by comparing different frame joints including bolted joints, bonded joints and hybrid joints. The stiffness of the structure can be enhanced by appropriate design of the connections. Modeling methods of the composite joints in the FEM are studied and verified by experiments. This paper offers an important reference to the design, test, and simulation of composite cabin structure in spacecraft.

1 Experimental investigation

1.1 Design and manufacture

The composite structure with frame and skin is designed according to the structural feature of cabin in a large space telescope as shown in Fig. 1. The structure is 0.8 m in width and 1.6 m in length. The frame consists of two longitudinal beams and three transverse beams connected by M6 bolts and J133 adhesive, thus forming six hybrid bonded/bolted joints. The frame joints in different parts can be classified into two types, namely, sleeve type at the end of longitudinal beams and groove type in the middle of longitudinal beams. Owing to such matching surfaces in the joints, the longitudinal and transverse beams can be assembled more easily and the strength of the joints is enhanced with more bonding interfaces compared with common lap joints. Five bonding interfaces and 16 bolts can be found in a joint of sleeve type, and four bonding interfaces and 10 bolts can be found in a joint of groove type. In accordance with the cabin structure design, the skin is connected to frame by bolts and anchor nuts, making it convenient to add or remove skin during the

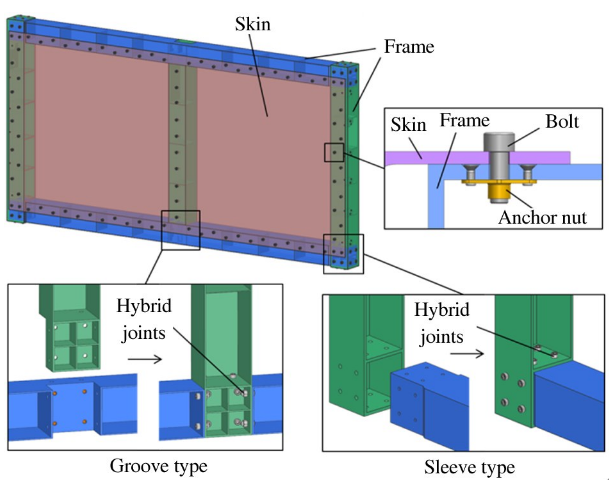

Fig. 1 Composite structure with multi hybrid joints

assembly and adjustment of space telescope. Eighty-eight pairs of M6 bolts and anchor nuts are used in this composite structure. The spacings of bolts in frame joints are 40 – 50 mm and those of skin-frame bolts are 60 – 70 mm, ensuring that the spacings are 5 times larger than the diameter of bolts to avoid damage to the composite strength[4].

The composite laminates used for frame and skin are made of carbon fiber T800 and cyanate ester, and all M6 bolts are made of stainless steel 1Cr18Ni9Ti. The material properties of T800/cyanate unidirectional plate are listed in Table 1, and the elastic properties of 1Cr18Ni9Ti and J133 are listed in Table 2.

Table 1 Material properties of T800/cyanate unidirectional plate

Material property	Value
E_1 /GPa	160
E_2 /GPa	9
$G_{12} = G_{13}$ /GPa	4
G_{23} /GPa	3.17
v_{12}	0.3
ρ /(kg/m^3)	1650

Note: E_1 - Elastic modulus in longitudinal direction (fiber direction)
E_2 - Elastic modulus in lateral direction
G_{ij} - Shear modulus in $i-j$ plane
v_{12} - Poisson's ratio
ρ - Mass density

Table 2 Elastic properties of 1Cr18Ni9Ti and J133

Elastic property	1Cr18Ni9Ti	J133
E /GPa	206	1.85
v	0.3	0.33

Note: E - Elastic modulus v - Poisson's ratio

The composite structure is manufactured with T800/cyanate prepreg, and the thickness of the prepreg is 0.2 mm. The thicknesses and ply stacking sequences of different parts in the structure are shown in Table 3.

Table 3 Ply stacking sequences of composite parts

Part	Thickness /mm	Stacking sequence
Longitudinal beams	2.2	[0/90/0/0/45/-45/0/-45/45/0/0]
Transverse beams at ends	4.2	[0/45/90/-45/0/0/45/90/-45/0/45/90/-45/-45/90/45/0/-45/90/45/0]
Transverse beam in the middle	2	[0/90/0/45/90/-45/-45/90/45/0]
Skin	2	[0/45/90/-45/0/90/-45/90/45/0]

During the manufacturing process, the clearance between bonding surfaces of frame joints is controlled at about 0.1 mm, which is the adhesive thickness. The J133 adhesive has the largest strength at the thickness of 0.1 – 0.2 mm according to the research of Ref. [19]. The joint surfaces are cleaned before bonding, and M6 bolts are used to connect the joints during bonding. After the curing of the adhesive at room temperature, flaw detection is conducted on the joints to ensure that the effective bonding area ratio of the bonding surfaces is above 90%. The assembly and bonding process of the composite structure is shown in Fig. 2.

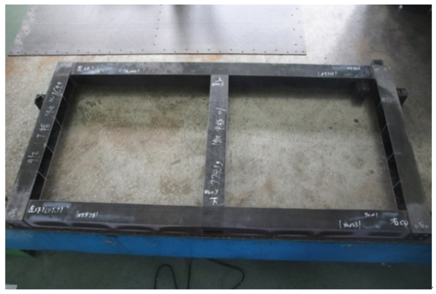

(a) Assembly of frame before bonding

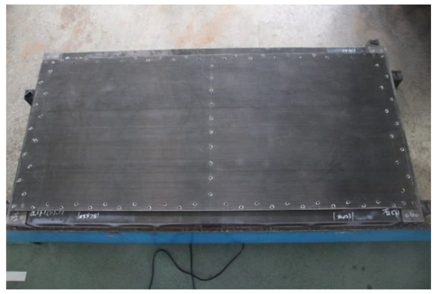

(b) Assembly of skin and frame

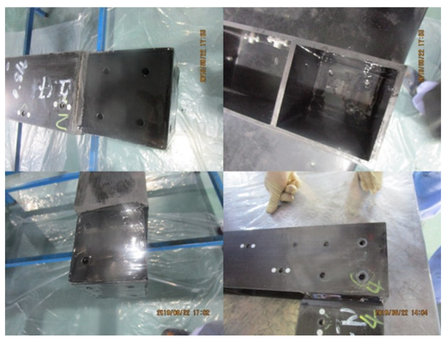

(c) Adhesive bonding

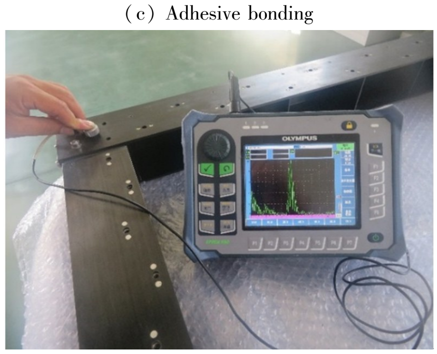

(d) Flaw detection after bonding

Fig. 2 Assembly and bonding process

1.2 Experimental tests and analysis

The composite structure is a local structure in the cabin of a space telescope. The whole cabin structure is simulated in the case of extreme load during launch, and the tensile load with maximum value of 30 kN on the interface of the composite structure is achieved.

A test stand is built for the tensile tests of the composite structure as shown in Fig. 3. A trapezoidal block made of steel is connected to one transverse beam at the end of the structure by six M10 bolts to uniformly disperse the load on the beam. The loading point is closer to the surface of frame covered with skin than the other surface to reduce the warping of the structure caused by eccentric loading. The transverse beam at the other end of the structure is connected to a baseplate made of steel by six M10 bolts, and the baseplate is fixed on the ground. Twelve metal pieces are added to the inner sides of the transverse beams at both ends of the structure to connect all the M10 bolts. A hydraulic actuator is used to apply load on the trapezoidal block along the direction of longitudinal beam, which is defined as X direction.

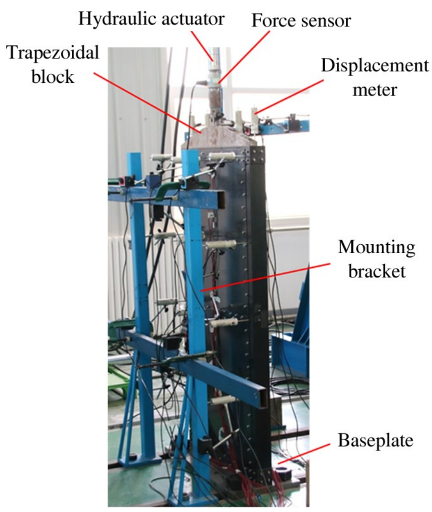

Fig. 3 Test stand of the composite structure

Sixteen displacement meters and eighteen cross stain gauges are used in the tests, and their distribution is shown in Fig. 4, where Nos. 1 – 16 indicate the displacement measurement points, and Nos. $Y1$ – $Y18$ indicate the strain measurement points. Cross stain gauges are used to measure strains in X and Y directions (along the direction of transverse beam) as shown in Fig. 5. All the measurement data are collected by equipment DH3816N, a test and analysis system of static stress and strain. The specifications of experimental equipment used in the tests are listed in Table 4.

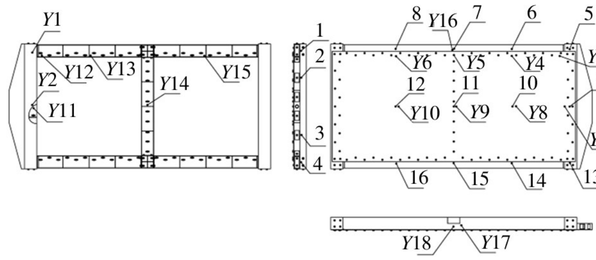

Fig. 4 Distribution of measurement points

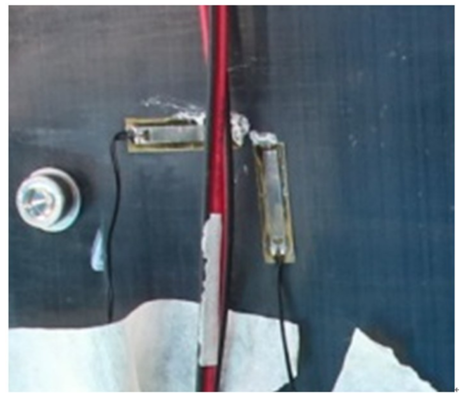

Fig. 5 Cross strain gauges used

Table 4 Specifications of experimental equipment

Equipment	Specification
Hydraulic actuator	Range: 10 t
Force sensor	Range: 10 t Measurement accuracy: 0.02%
Displacement meter	Range: 30 mm; Linearity error: <0.5% (F. S)
Strain gauge	Resistance value: 120 Ω; Sensitive coefficient: 2.03
Data acquisition system	72 channels max

In the tensile tests, load is applied with increment of 2 kN until the maximum value of 30 kN is achieved. The load is then decreased with increment of 2 kN until the value reaches zero. After the first tensile test, a second tensile test is conducted repeatedly. The tightening torque of the bolts connecting the skin and frame is 8 N · m in the two tests. The X-direction displacement curves of point 2 on the loading beam are shown in Fig. 6, and the strain curves of point $Y8$ in the center of the skin are shown in Fig. 7.

The values of displacement and stains at the first test differ from those at the second test and fail to reach zero in the first test when the structure is totally unloaded but become zero in the second test. Thus, residual deformation exists in the first test but disappears in the following tests of the structure. Given that the curves of displacements and strains are generally linear and the structure is not damaged, the above problem can be attributed to the bolted connection of the skin and frame because of the clearances between M6 bolt shanks and bolt holes with diameter of 6.5 mm.

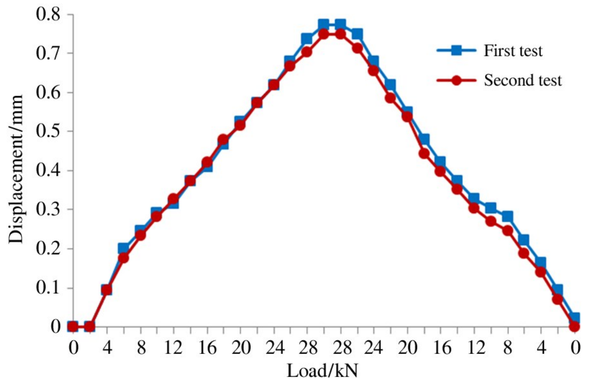

Fig. 6 Displacement curves of point 2 in composite structure

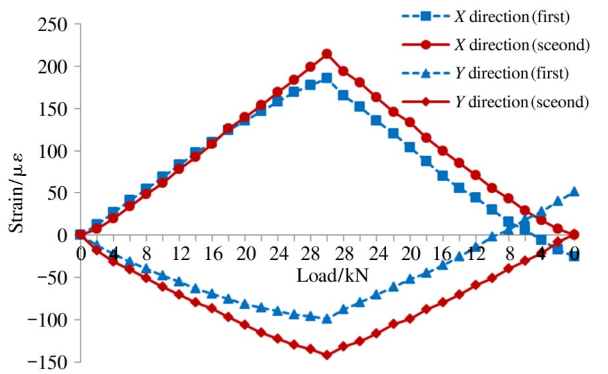

Fig. 7 Strain curves of point *Y*8 in composite structure

Another contrast test of frame only is conducted as shown in Fig. 8. The maximum tensile load is 24 kN, under which the displacement of the frame is close to the maximum displacement of the structure with skin. The *X*-direction displacement curve of point 2 on loading beam is shown in Fig. 9, and the strain curves of point *Y*13 on longitudinal beam are shown in Fig. 10. All the curves are linear and symmetrical during loading and unloading, and the values of displacement and stains become zero when the structure is totally unloaded.

Fig. 8 Tensile test of the frame only

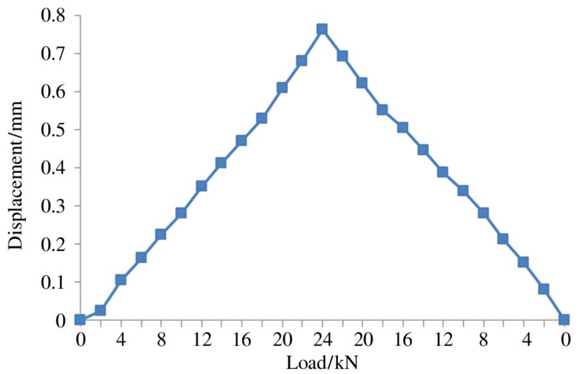

Fig. 9 Displacement curve of point 2 in frame

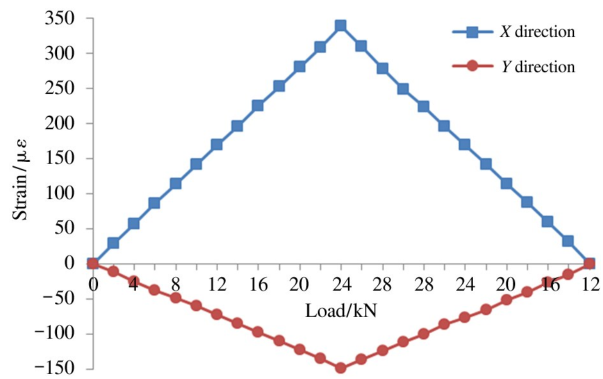

Fig. 10 Strain curves of point *Y*13 in frame

For the structure with skin, when the structure is loaded for the first time, the skin initially takes some load by friction with frame. When the load transferred by the skin exceeds the maximum static friction force with the frame, the skin slides relatively to the frame so that the bolt shanks contact the bolt holes to directly take shear load. When the structure is unloaded, the relative displacement between the skin and frame generates resistance against the structure deformation, resulting in the asymmetry of curves in the first test. The relative displacement remains when the structure is totally unloaded at the first time. When the structure is loaded at the second time, the residual relative displacement causes the bolt shanks to contact the bolt hole to take the shear load, resulting in the lack of residual deformation when the structure is totally unloaded at the second time. For the frame only with hybrid bonded/bolted joints, the hybrid joints take the load with no such relative displacement.

The maximum X-direction displacement of point 2 is 0.77 mm in the first test and 0.75 mm in the second test. Such relative displacement between the skin and frame resulting from bolted connection reduces the stiffness of the structure, but the effect is not serious.

More tensile tests are conducted with the tightening torques of the skin-frame bolts at 4 N · m and 9 N · m, and two tests are conducted for each case. The same phenomenon is observed: residual deformation occurs in the first test but disappears in the following tests. However, the residual deformation for 9 N · m is rather small. The X-direction displacement curves of point 2 with different bolt tightening torques are shown in Fig. 11. A high bolt tightening torque contributes to the high stiffness of the structure because it generates a high friction force between the skin and frame, resulting in large load transfer capacity of skin and reduction in the relative displacement between the skin and frame.

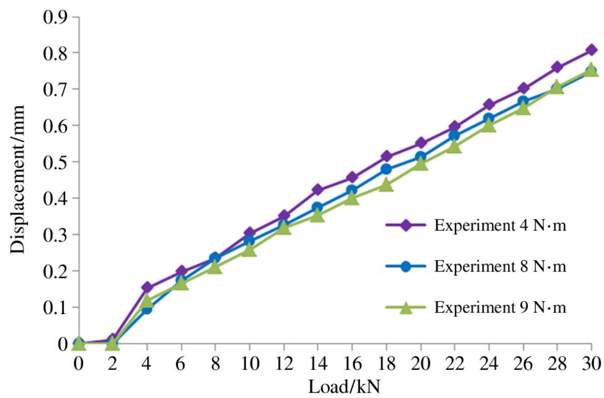

Fig. 11 Displacement curves of point 2 with different tightening torques of skin-frame bolts

Further tensile tests are conducted with half the number of the skin-frame bolts at tightening torque of 8 N · m as shown in Fig. 12. The X-direction displacement curves of point 2 with different numbers of skin-frame bolts are shown in Fig. 13. Increased number of bolts also contributes to the high stiffness of the structure because it can increase the friction force between the skin and frame.

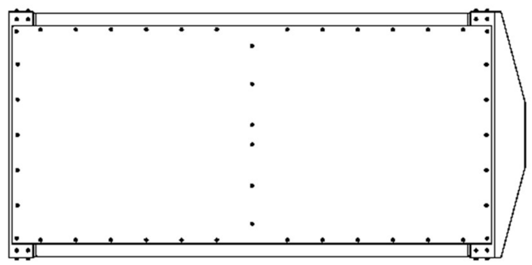

Fig. 12 Distribution of skin-frame bolts with half the number

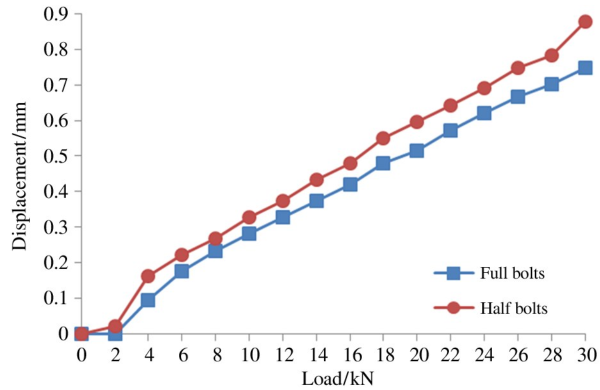

Fig. 13 Displacement curves of point 2 with different numbers of skin-frame bolts

2 Numerical investigation

2.1 Established FEM

The finite element analysis of this composite structure is conducted by Hyperworks platform. The FEM is established by Hypermesh as shown in Fig. 14. Six degrees of freedom of the four bolt holes of the baseplate are constrained. Load is applied on the central point on the top of trapezoidal block. The composite parts are modeled by 2D shell elements because of their thin-shell structure. The trapezoidal block and baseplate are modeled by 3D solid elements. Given that the model contains details, such as bolt holes, the types of elements are set as mixed. The general size of the elements in the frame and trapezoidal block is 4 mm, and that in the skin and baseplate is 6 mm. There are 236 634 elements and 250 307 nodes in the FEM.

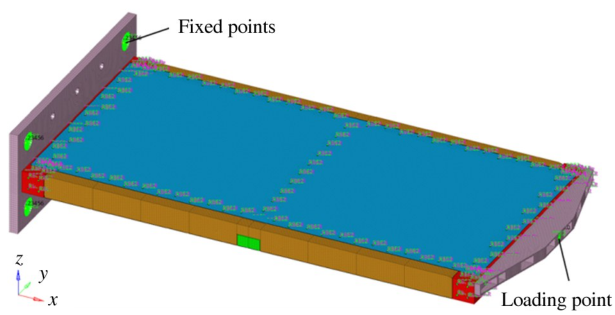

Fig. 14 Finite element model of the composite structure

Given that bolted and adhesive connections are crucial to the mechanical performance of the structure, their accurate modeling methods in the FEM are important. The bolt connecting the two surfaces is modeled by CBAR element, which connects the two centers of bolt holes. The holes' centers are connected to the nodes on the holes' edges by RBE2 elements as shown in Fig. 15. The CBAR element is assigned with material properties and diameters of connecting bolt. The adhesive layer in composite joints is modeled by a layer of sold elements with thickness of 0.1 mm as shown in Fig. 16. The adhesive elements are connected to the bonding surfaces by RBE3 elements.

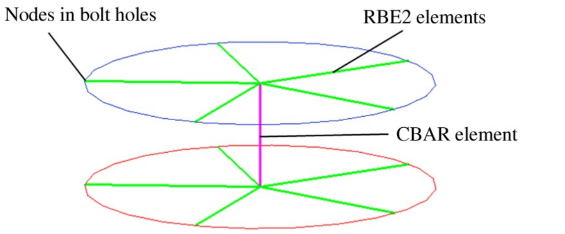

Fig. 15 Modeling of bolted connection

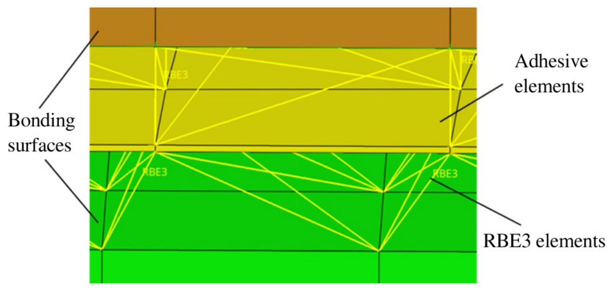

Fig. 16 Modeling of adhesive connection

2.2 Finite element analysis

The FEM of the composite structure is analyzed with the type of linear static by OptiStruct and postprocessed by Hyperview. The contour plots of X-direction displacement and element stresses of the composite structure under the maximum load of 30 kN are shown in Figs 17 and 18, respectively. The maximum displacement in the structure occurs in the middle of loading beam. The largest stress in the structure is 122.5 MPa, indicating that the structure is not damaged.

The X-direction displacement curves of point 2 on the loading beam are shown in Fig. 19 with the comparison of experimental results with different tightening torques of the skin-frame bolts. The FEM results of the structure show better agreement with the experimental results for the high tightening torque of the skin-frame bolts. In particular, the experimental results with 9 N · m

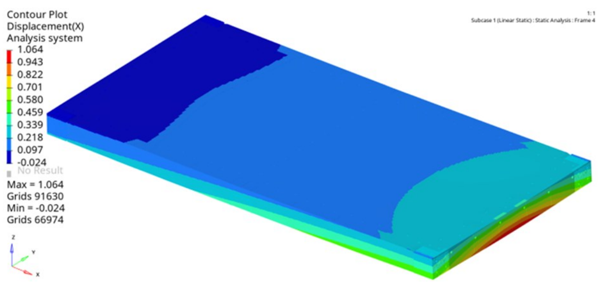

Fig. 17 Contour plot of X-direction displacement

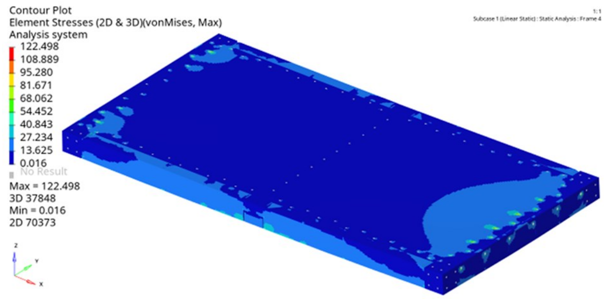

Fig. 18 Contour plot of element stresses

bolt tightening torque are quite close to the numerical simulation results. Given that the bolt-hole clearance is not considered in the FEM, the relative displacement between the skin and frame cannot be simulated. Meanwhile, the effect of bolt-hole clearance is reduced by increasing the bolt tightening torque in the experimental tests.

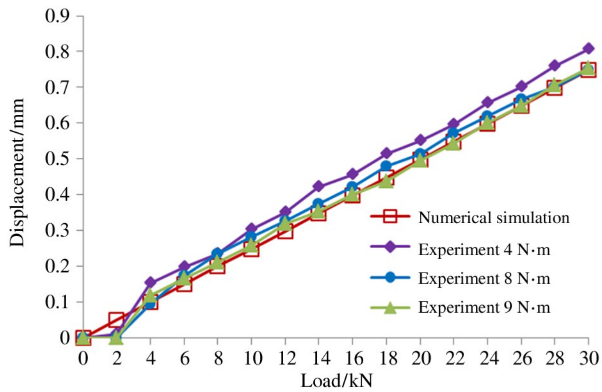

Fig. 19 Displacement curves of point 2 with comparison of simulation and experimental results

The displacements under a small load of 2 kN in the experimental tests are smaller than those in the numerical simulation (0.05 mm). This finding can be attributed to the measurement error of displacement meter, which is installed with long cantilever and generates error under such small displacement.

The FEM of this structure is contrastively analyzed where the frame is connected by adhesive only or bolts only. The X-direction displacement curves of point 2 are shown in Fig. 20. The FEM results with hybrid joints are nearly identical to those with bonded joints but differ from those with bolted joints. The stiffness values of the composite structures with hybrid joints, bonded joints, and bolted joints are 40.14 kN/mm, 39.95 kN/mm, and 31.54 kN/mm, respectively. The stiffness of the structure with hybrid joints is 27% higher than that of the structure with bolted joints. Therefore, the adhesive plays a leading role in the stiffness performance of hybrid joint in an undamaged structure.

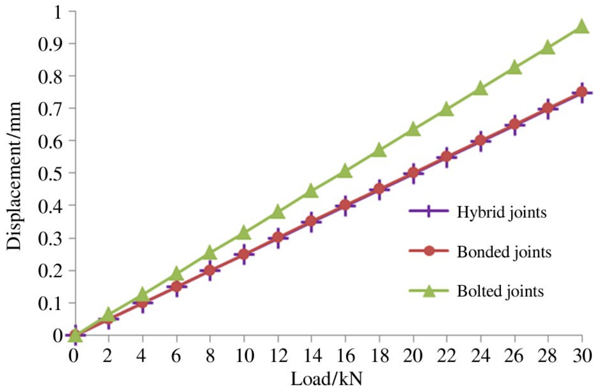

Fig. 20 Displacement curves of point 2 with different joints

Given that the adhesive plays a leading role in the stiffness of hybrid joint, a simplified modeling method that only considers adhesive can be adopted. Tie contacts are used between the bonding surfaces of frame in FEM as shown in Fig. 21. The Tie contacts in the FEM are defined by using the MPC-based method, which enforces zero relative motion at the interfaces. The *X*-direction displacement curves of point 2 of FEM with Tie contacts are shown in Fig. 22, and the experimental results for the bolt tightening torque of 9 N · m are shown for comparison. The figure shows that the FEM with Tie contacts can accurately simulate the stiffness performance of the structure in an undamaged situation.

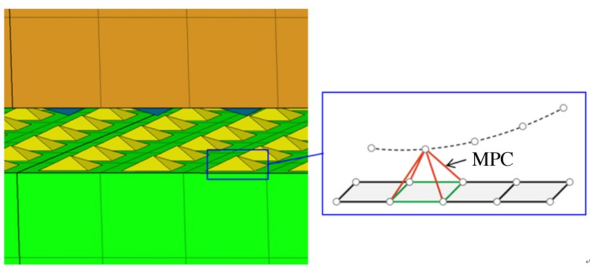

Fig. 21 Tie contacts in finite element model

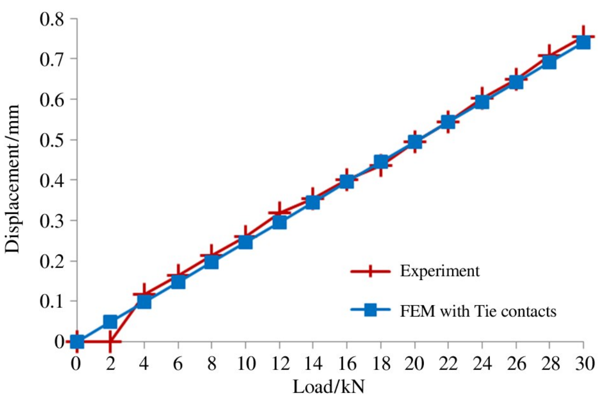

Fig. 22 Displacement curves of point 2 with Tie contacts

3 Conclusion

In this work, a composite structure with frame and skin based on the cabin structure in a large space telescope is manufactured and investigated. The frame is composed of beams with hybrid bonded/bolted joints, and the skin is connected to the frame by bolts. Experimental tests and finite element analyses are conducted on the prepared composite structure. Conclusions are drawn as follows.

(1) Tensile tests reveal that the residual deformation of the structure occurs in the first test but does not occur for frame only. This phenomenon is attributed to the bolt-hole clearances of the bolted connections of the skin and frame, resulting in relative sliding when the load transferred in the skin exceeds the maximum static friction force and in the slightly reduced stiffness of the structure.

(2) The high tightening torque and the increased number of the skin-frame bolts contribute to the high stiffness of the structure because the increased friction force between the skin and frame leads to large load transfer capacity of the skin and the reduced relative displacement of the skin and frame.

(3) The analysis results of the FEM of the structure with modeling of bolted connection and adhesive connection show a good agreement with the experimental results. Results of contrastive analyses with different frame joints indicate that the stiffness of the structure with hybrid bonded/bolted joints is obviously higher than that of the structure with bolted joints, and the adhesive plays a leading role in the stiffness of hybrid joints.

(4) A simplified modeling method of Tie contacts in FEM is proposed to simulate bonded or hybrid bonded/bolted joints when studying the stiffness performance of undamaged structures.

References

[1] NORKHAIRUNNISA M, SAPUAN S M, ILYAS R A. Advanced composites in aerospace engineering applications[M]. Cham: Springer, 2022: 1-21.
[2] SHI W, GAO F, CHAI H. Application and expectation of composite in spacecraft structure[J]. Aerospace Materials and Technology, 2019, 4: 1-6. (In Chinese)
[3] YI X S, DU S, ZHANG L. Composite materials engineering, volume 1[M]. Singapore: Springer, 2018: 461-509.
[4] SHEN Z. Design handbook for composite structures[M]. Beijing: Aviation Industry Publisher, 2001: 145-190. (In Chinese)
[5] ZHANG H, ZHANG L, LIU Z, et al. Numerical analysis of hybrid (bonded/bolted) FRP composite joints: a re-

view[J]. Composite Structures, 2021,262(2):113606.

[6] MCCARTHY M A, LAWLOR V P, STANLEY W F, et al. Bolt-hole clearance effects and strength criteria in single-bolt, single-lap, composite bolted joints[J]. Composites Science and Technology, 2002,62(10-11):1415-1431.

[7] MCCARTHY C T, MCCARTHY M A, LAWLOR V P. Progressive damage analysis of multi-bolt composite joints with variable bolt-hole clearances[J]. Composites Part B Engineering, 2005,36(4):290-305.

[8] MCCARTHY M A, MCCARTHY C T, LAWLOR V P, et al. Three-dimensional finite element analysis of single-bolt, single-lap composite bolted joints: part I: model development and validation[J]. Composite Structures, 2005, 71: 140-158.

[9] MCCARTHY C T, MCCARTHY M A. Three-dimensional finite element analysis of single-bolt, single-lap composite bolted joints: part II: effects of bolt-hole clearance [J]. Composite Structures, 2005, 71: 159-175.

[10] SUN H T, CHANG F K, QING X. The response of composite joints with bolt-clamping loads, part I: model development[J]. Journal of Composite Materials, 2002, 36(1): 47-67.

[11] SUN H T, CHANG F K, QING X. The response of composite joints with bolt-clamping loads, part II: model verification[J]. Journal of Composite Materials, 2002, 36(1): 69-92.

[12] LI X, TAN Z, WANG L, et al. Experimental investigations of bolted, adhesively bonded and hybrid bolted/bonded single-lap joints in composite laminates[J]. Materials Today Communications, 2020, 24: 101244.

[13] BARUT A, MADENCI E. Analysis of bolted-bonded composite single-lap joints under combined in-plane and transverse loading[J]. Composite Structures, 2009, 88(4): 579-594.

[14] LEE Y H, LIM R W, CHOI R H, et al. Failure load evaluation and prediction of hybrid composite double lap joints[J]. Composite Structures, 2010, 92(12): 2916-2926.

[15] KWEON J H, JUNG J W, KIM T H, et al. Failure of carbon composite-to-aluminum joints with combined mechanical fastening and adhesive bonding[J]. Composite Structures, 2006, 75(1): 192-198.

[16] GAMDANI F, BOUKHILI R, VADEAN A. Tensile behavior of hybrid multi-bolted/bonded joints in composite laminates[J]. International Journal of Adhesion and Adhesives, 2019, 95(11): 102426.

[17] LI X, CHENG X, CHENG Y, et al. Tensile properties of a composite-metal single-lap hybrid bonded/bolted joint [J]. Chinese Journal of Aeronautics, 2020, 34(2): 629-640.

[18] ZHANG C. Tensile properties of composite multi-nail hybrid joints and fatigue life research[D]. Zhengzhou: Zhengzhou University, 2021. (In Chinese)

[19] CUI Y, HE X, ZHANG K. Technique of cementation between the titanium alloys and carbon fibers[J]. Optical Technique, 2012, 38(1): 125-128. (In Chinese)

LI Chuanzheng, born in 1988. He is a research assistant and Ph. D candidate in Changchun Institute of Optics, Fine Mechanics and Physics, Chinese Academy of Sciences. He received his B. S. and M. S. degrees from Northwestern Polytechnical University in 2012 and 2015 respectively. His research interests include the structure design of space telescope.